

# Aromaticity of Planar $B_5^-$ Anion in the $MB_5$ ( $M = Li, Na, K, Rb,$ and $Cs$ ) and $MB_5^+$ ( $M = Be, Mg, Ca,$ and $Sr$ ) Clusters

Qian Shu Li\* and Qiao Jin

School of Science, Beijing Institute of Technology, Beijing 100081, P. R. China

Received: September 11, 2003; In Final Form: November 20, 2003

The ground-state geometries, electronic structures, and vibrational frequencies of alkali metal– $B_5^-$   $MB_5$  ( $M = Li, Na, K, Rb,$  and  $Cs$ ) and alkaline earth metal– $B_5^-$   $MB_5^+$  ( $M = Be, Mg, Ca,$  and  $Sr$ ) clusters were investigated using ab initio self-consistent field and density functional theory (DFT) methods. Calculation results show that planar  $B_5^-$  anion can coordinate with the metal atom to form metal–polyboron  $MB_5$  and  $MB_5^+$  species. On the basis of the molecular orbital (MO) analysis and nucleus-independent chemical shifts (NICS), we revealed that the planar  $B_5^-$  anion exhibits characteristic of  $\pi$ -aromaticity with two delocalized  $\pi$  electrons and maintains its structural and electronic integrity inside the five  $MB_5$  and four  $MB_5^+$  clusters.

## 1. Introduction

In 1988, Anderson and co-workers<sup>1</sup> observed the mass distribution of  $B_n^+$  ( $n = 1-20$ ) generated by laser ablation of isotopically pure solid boron. The collision-induced dissociation (CID) results revealed the presence of “magic”  $n = 5$  and 13 clusters that exhibited anomalously high intensity. The results of Anderson’s group<sup>2–5</sup> inspired theoretical investigation of small bare boron clusters<sup>6–20</sup> and especially  $B_5$  and  $B_5^+$  clusters, whereas a few of theoretical investigations have been reported on the  $B_5^-$  cluster. Until recently, we theoretically investigated structures and energetics of neutral, cationic, and anionic  $B_4^{17}$  and  $B_5^{18}$  clusters with the MP2/6-311+G\* and B3LYP/6-311+G\* levels of theory. Zhai et al.<sup>21</sup> investigated the electronic structure and chemical bonding of  $B_5^-$  and  $B_5$  using anion photoelectron spectroscopy and ab initio calculations. Excellent agreement between the ab initio detachment energies of the  $C_{2v}$  global minimum of  $B_5^-$  and the experimental PES spectra firmly established the ground-state structures for both  $B_5^-$  and  $B_5$ .

The concept of aromaticity has been successfully extended from traditional organic molecules into pure all-metal clusters.<sup>22–31</sup> Li and co-workers<sup>22</sup> presented evidence of aromaticity for  $MA_4^-$  ( $M = Li, Na,$  and  $Cu$ ) purely metallic systems. The  $Al_4^{2-}$  dianion in a series of bimetallic clusters was found to have two delocalized  $\pi$  electrons conforming to the  $4n + 2$  electron counting rule for aromaticity.  $Ga_4^{2-}$  and  $In_4^{2-}$  dianions<sup>23</sup> inside the gaseous  $NaGa_4^-$  and  $NaIn_4^-$  clusters also have similar aromaticity due to the presence of two delocalized  $\pi$  electrons. Li et al.<sup>24</sup> investigated the possibility of aromaticity in the heterocyclic four-membered ring  $XAl_3^-$  ( $X = Si, Ge, Sn,$  and  $Pb$ ) systems and found that the cyclic planar  $XAl_3^-$  species have delocalized  $\pi$  electrons and therefore aromaticity. Aromaticity was also proposed in the 10 valence electrons  $B_3^-, Al_3^-,$  and  $Ga_3^-$  systems to explain the geometrical and electronic properties.<sup>25</sup> Li and Cheng<sup>32</sup> investigated the aromaticity of square planar  $N_4^{2-}$  (possessing six delocalized  $\pi$  electrons) in the  $M_2N_4$  ( $M = Li, Na, K, Rb,$  or  $Cs$ ) species. Boldyrev and Wang<sup>33</sup> reported the experimental and theoretical characterization of antiaromaticity in an all-metal system  $Li_3Al_4^-$ . Molecular orbital analysis revealed that the rectangular  $Al_4^{4-}$  tetraanion has four

$\pi$  electrons, consistent with the  $4n$  Hückel rule for antiaromaticity.

In the present paper, a series of alkali metal– $B_5^-$   $MB_5$  ( $M = Li, Na, K, Rb,$  and  $Cs$ ) and alkaline earth metal– $B_5^-$   $MB_5^+$  ( $M = Be, Mg, Ca,$  and  $Sr$ ) clusters are theoretically investigated using ab initio and DFT methods. We explored the aromaticity of planar  $B_5^-$  anion in the five  $MB_5$  and four  $MB_5^+$  species. Molecular orbitals (MO) analysis and the nucleus-independent chemical shifts (NICS) provide insight into the aromaticity of planar  $B_5^-$  anion. Our results show that the inorganic  $B_5^-$  anion exhibits characteristic  $\pi$ -aromaticity having two delocalized  $\pi$  electrons with structural and magnetic criteria.

## 2. Computational Methods

All calculations were performed using the Gaussian 98 program package.<sup>34</sup> Equilibrium geometries and vibrational frequencies of  $B_5^-$ ,  $MB_5$  ( $M = Li, Na, K, Rb,$  and  $Cs$ ), and  $MB_5^+$  ( $M = Be, Mg, Ca,$  and  $Sr$ ) were fully optimized using the B3LYP and MP2 methods, where MP2 stands for the second-order Møller–Plesset perturbation theory,<sup>35</sup> and B3LYP is a DFT method using Becke’s three parameter nonlocal exchange functional<sup>36</sup> with the nonlocal correlation functionals of Lee, Yang, and Parr.<sup>37</sup> The 6-311+G\* is a split-valence triple- $\zeta$  plus polarization basis set augmented with diffuse functions.<sup>35</sup> For the  $RbB_5$ ,  $CsB_5$ , and  $SrB_5^+$  species, we optimized at the B3LYP and MP2 levels of theory, whereas the 6-311+G\* basis set was used for boron and the lighter metal atoms and the LANL2DZ basis set was used for the heavier metals Rb ( $Z = 37$ ), Cs ( $Z = 55$ ), and Sr ( $Z = 38$ ). Vibrational frequencies at the above levels were calculated to characterize stationary points as minima (number of imaginary frequencies (NIMAG = 0)) or transition states (NIMAG = 1).

Molecular orbitals (MO) for  $B_5^-$ ,  $BeB_5^+$ , and  $LiB_5$  were calculated by the HF methods with the corresponding basis set. All MO pictures were made using the MOLDEN 3.4 program.<sup>38</sup> NICS values for  $B_5^-$  anion, five  $MB_5$ , and four  $MB_5^+$  species were calculated with the GIAO-B3LYP//B3LYP method. The natural bond orbital (NBO)<sup>39–42</sup> analysis is also performed to provide insight into the bonding nature and aromaticity of these species.

\* Corresponding author. Fax: +86-10-68912665. E-mail: qqli@bit.edu.cn.

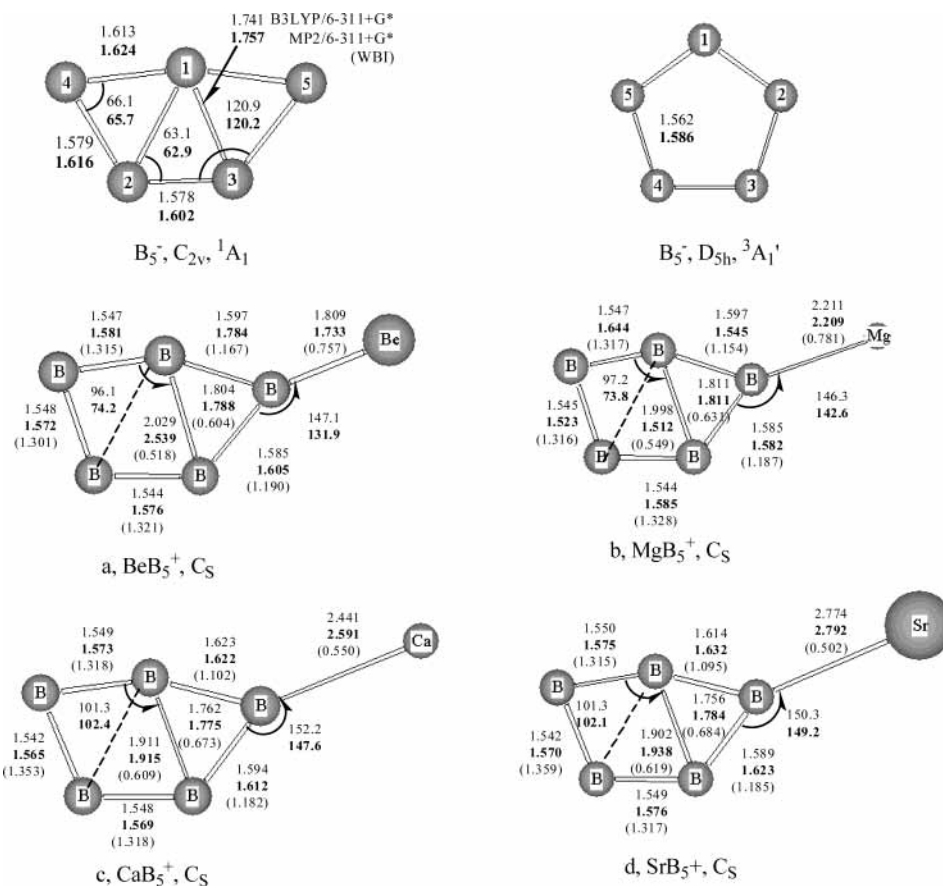


**Figure 1.** Optimized geometries (bond lengths in Å, bond angles in degrees) and the Wiberg bond indices (WBI) for  $BeB_5^+$ ,  $MgB_5^+$ ,  $CaB_5^+$ , and  $SrB_5^+$  species at the B3LYP and MP2 (bold font) methods.

### 3. Results and Discussion

The optimized geometric structures and the Wiberg bond indices (WBI) for  $B_5^-$  anion, five  $MB_5$ , and four  $MB_5^+$  species were shown in Figures 1 and 2. Total energies, ZPE, and the number of imaginary frequencies of all species are summarized in Table 1. The calculated average bond lengths (in Å), covalent radii (in Å), and zero-point corrected B3LYP energies (in kcal/mol) for hypothetical reactions  $MB_5 \rightarrow M + B_5$  or  $MB_5^+ \rightarrow M^+ + B_5$  are listed in Table 2. The harmonic vibrational frequencies of  $B_5^-$ , five  $MB_5$ , and four  $MB_5^+$  species at the B3LYP method are shown in Table 3. The calculated NICS values are given in Table 4. MOs pictures for  $B_5^-$ ,  $BeB_5^+$ , and  $LiB_5$  are exhibited in Figure 3.

#### 3.1. Geometric Structures and Optimized Bond Lengths.

Extensive searches were carried out for the most stable structure of  $B_5^-$  at the B3LYP/6-311+G\* and MP2/6-311+G\* levels of theory. Theoretical studies on various  $B_5^-$  anions showed that a  $C_{2v}$  planar five-membered ring structure is the global minimum of  $B_5^-$ , in good agreement with previous results.<sup>18,21</sup> The most stable structure of the  $B_5^-$  anion ( $C_{2v}$ ,  $^1A_1$ ) is a Jahn–Teller distorted pentagon. To understand this distortion, the triplet  $B_5^-$  structure with the  $D_{5h}$  symmetry must be considered. The pentagonal  $B_5^-$  anion ( $D_{5h}$ ,  $^3A_1'$ ) is a second-order saddle point at the B3LYP/6-311+G\* level of theory, whereas it is a local minima at the MP2/6-311+G\* level of theory. The triplet  $B_5^-$  ( $D_{5h}$ ) anion is energetically higher than the most stable  $B_5^-$  anion ( $C_{2v}$ ,  $^1A_1$ ) by 87.1 kcal/mol at the MP2/6-311+G\* level of theory (shown in Table 1).

We performed ab initio and DFT methods on a wide variety of metal–polyboron clusters and found that all the ground-state  $MB_5$  and  $MB_5^+$  geometries are local minima with all real

**TABLE 1: Total Energies ( $E$ ),<sup>a</sup> Zero-Point Energies (ZPE),<sup>b</sup> and the Number of Imaginary Frequencies (NIMAG) for  $B_5^-$ ,  $MB_5^+$ , and  $MB_5$  Species<sup>c–e</sup>**

species	B3LYP		MP2		RE <sup>f</sup>
	E <sup>a</sup>	ZPE <sup>b</sup>	E <sup>a</sup>	ZPE <sup>b</sup>	
$B_5^-$ $C_{2v}$ , $^1A_1$	−124.080871	9.8(0)	−123.619033	9.7(0)	0.0
$B_5^-$ $D_{5h}$ , $^3A_1'$	−123.973339	8.4(2)	−123.480303	29.3(0)	87.1
$BeB_5^+$ $C_e$	−138.456963	11.4(0)	−137.929887	11.4(0)	0.0
$MgB_5^+$ $C_{5v}$			−137.778721	11.7(2)	94.8
$MgB_5^+$ $C_e$	−323.879458	10.9(0)	−322.835606	9.8(2)	0.0
$MgB_5^+$ $C_{5v}$			−322.896608	11.2(0)	−38.3
$CaB_5^+$ $C_e$	−801.412904	10.7(0)	−800.094010	10.8(0)	0.0
$CaB_5^+$ $C_{5v}$	−801.361058	9.8(2)	−800.024951	11.9(0)	43.3
$SrB_5^+$ $C_e$	−154.261629	10.7(0)	−153.507621	10.4(0)	0.0
$SrB_5^+$ $C_{5v}$	−154.182747	9.4(2)	−153.435802	12.1(0)	45.1
$LiB_5$ $C_e$	−131.564901	10.1(0)	−131.014821	10.9(0)	0.0
$LiB_5$ $C_{5v}$	−131.503173	10.2(2)	−130.985829	12.8(0)	18.2
$NaB_5$ $C_e$	−286.342692	10.6(0)	−285.446434	10.3(0)	0.0
$NaB_5$ $C_{5v}$	−286.268458	9.5(2)	−285.372411	13.6(0)	46.5
$KB_5$ $C_e$	−723.984892	10.5(0)	−722.923548	10.5(0)	0.0
$KB_5$ $C_{5v}$	−723.912690	9.3(2)	−722.856391	14.9(0)	42.1
$RbB_5$ $C_1$	−147.914809	10.5(0)	−147.188303	10.3(0)	0.0
$RbB_5$ $C_{5v}$	−147.838185	9.1(2)	−147.100024	17.4(0)	55.4
$CsB_5$ $C_{2v}$	−143.931687	10.3(0)	−143.179111	10.5(0)	0.0
$CsB_5$ $C_{5v}$	−143.852969	9.0(2)	−143.123015	19.2(0)	35.2

<sup>a</sup> Total energies in Hartree. <sup>b</sup> Zero-point energies in kcal/mol. <sup>c</sup> The integers in parentheses are the number of imaginary frequencies (NIMAG). <sup>d</sup> The listed total energies for  $MB_5^+$  and  $MB_5$  species at the B3LYP and MP2 methods. <sup>e</sup> The 6-311+G\* basis set was used for boron, and the LANL2DZ basis set was used for Sr, Rb, and Cs. <sup>f</sup> Relative energies (in kcal/mol) for  $B_5^-$ ,  $MB_5^+$ , and  $MB_5$  species ( $C_e$  and  $C_{5v}$ ) at the MP2 method.

frequencies at the B3LYP and MP2 levels of theory. The metal atoms are lying in the five-membered ring plane bound to a boron atom of the five-membered ring. Planar  $B_5^-$  anion can

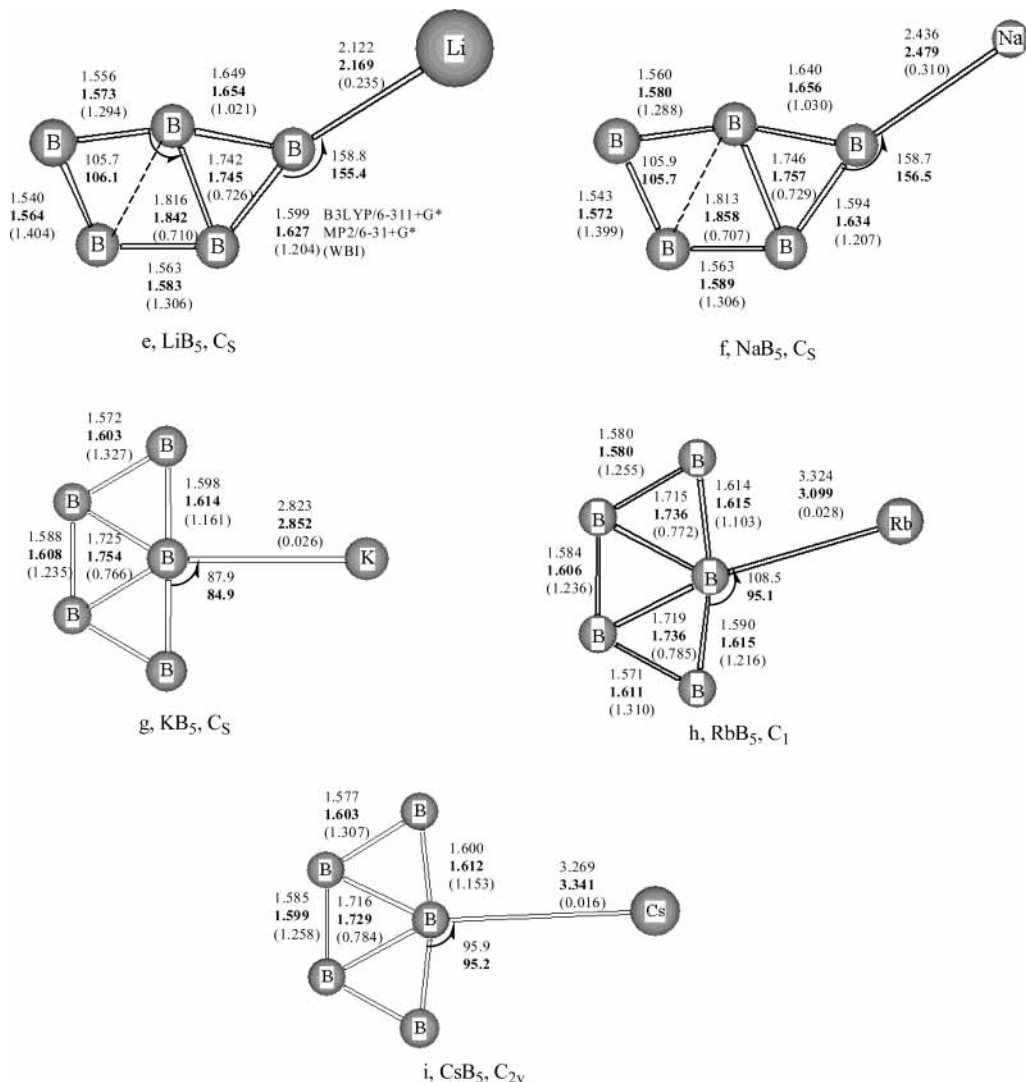


**Figure 2.** Optimized geometries (bond lengths in Å, bond angles in degrees) and the Wiberg bond indices (WBI) for  $LiB_5$ ,  $NaB_5$ ,  $KB_5$ ,  $RbB_5$ , and  $CsB_5$  species at the B3LYP and MP2 (bold font) methods.

**TABLE 2: Calculated Bond Lengths (in Å), Covalent Radii (in Å), and Zero-Point Corrected B3LYP Energies (in kcal/mol) for Hypothetical Reactions  $MB_5^+ \rightarrow M^+ + B_5$  or  $MB_5 \rightarrow M + B_5$**

species	$BeB_5^+$	$MgB_5^+$	$CaB_5^+$	$SrB_5^+$	$LiB_5$	$NaB_5$	$KB_5$	$RbB_5$	$CsB_5$
B–B	1.564	1.564	1.571	1.569	1.581	1.580	1.586	1.588	1.588
M–B	1.809	2.211	2.441	2.774	2.122	2.436	2.823	3.324	3.269
sum of covalent radii	1.77	2.25	2.62	2.79	2.10	2.45	2.90	3.04	3.23
$\Delta E$	73.8	42.1	37.6	28.7	44.3	33.2	34.9	30.3	32.3

coordinate with a metal atom to form metal–polyboron compounds  $MB_5$  and  $MB_5^+$ . Five  $MB_5$  and four  $MB_5^+$  species possess planar or quasi-planar structures containing the metal cation interacting with a planar  $B_5^-$  unit. Nine species have  $C_s$  symmetry except for the  $RbB_5$  ( $C_1$ ) and  $CsB_5$  ( $C_{2v}$ ) species.

In addition, we also have calculated the pentagonal pyramid structures  $MB_5$  and  $MB_5^+$  ( $C_{5v}$ ,  $^3A_1$ ) geometries. The triplet  $C_{5v}$   $MB_5^+$  ( $M = Mg, Ca, \text{ and } Sr$ ) clusters are local minima at the MP2/6-311+G\* level of theory. The triplet  $C_{5v}$   $MB_5$  ( $M = Li, Na, K, Rb, \text{ and } Cs$ ) clusters are second-order saddle points at the B3LYP/6-311+G\* level of theory and local minima at the MP2/6-311+G\* level of theory. They are energetically higher than the ground-state  $MB_5$  and  $MB_5^+$  geometries at the B3LYP/6-311+G\* and MP2/6-311+G\* levels of theory (shown in Table 1).

As shown in Figures 1 and 2, the bond lengths of B–B in the five  $MB_5$  and four  $MB_5^+$  species are slightly different using the B3LYP and MP2 methods. The B–B bond lengths (1.540–

**TABLE 3: Calculated Vibrational Frequencies (in  $cm^{-1}$ ) for the  $B_5^-$ ,  $MB_5^+$ , and  $MB_5$  Species**

species	B3LYP								
	$\omega_1$	$\omega_2$	$\omega_3$	$\omega_4$	$\omega_5$	$\omega_6$	$\omega_7$	$\omega_8$	$\omega_9$
$B_5^-$ ( $C_{2v}$ , $^1A_1$ )	253	374	581	638	718	964	997	1066	1258
$BeB_5^+$	124	142	238	335	380	535	663	757	1017
$MgB_5^+$	101	116	261	317	332	368	643	764	986
$CaB_5^+$	63	88	269	332	351	363	696	711	976
$SrB_5^+$	45	79	207	325	353	361	690	716	968
$LiB_5$	76	106	324	376	452	484	648	750	964
$NaB_5$	56	89	255	318	373	491	662	729	957
$KB_5$	56	64	208	292	386	604	682	748	988
$RbB_5$	48	96	159	247	387	618	664	747	991
$CsB_5$	38	54	129	246	388	618	662	751	994

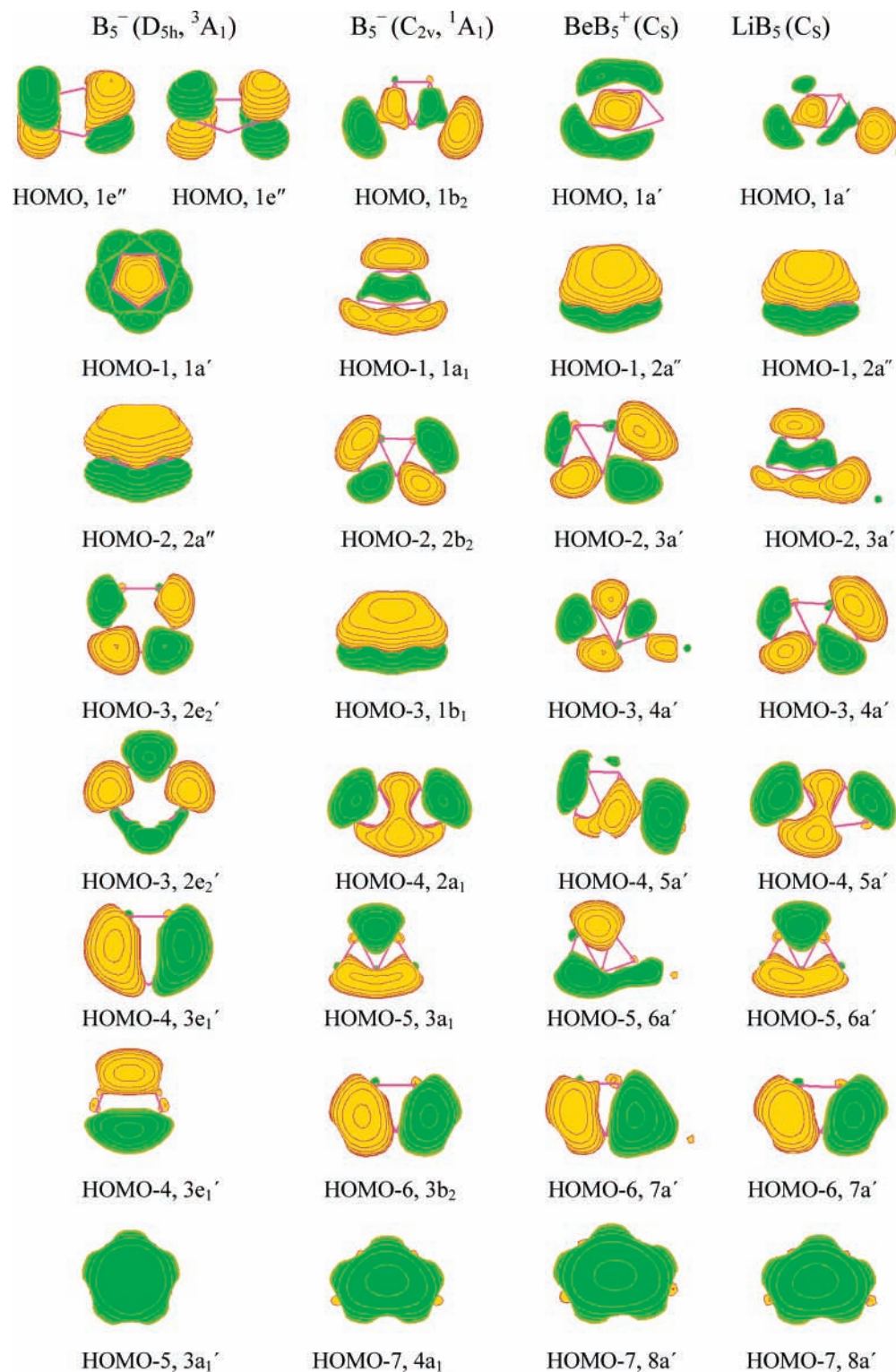
<sup>a</sup> The 6-311+G\* basis set was used for B, Be, Mg, Ca, Li, Na, and K, and the LANL2DZ basis set was used for the heavier metals Sr, Rb, and Cs.

1.754 Å) in the five  $MB_5$  and four  $MB_5^+$  species are much shorter than the sum of covalent radii of boron (1.76 Å),

**TABLE 4: NICS Values (in ppm) for the  $B_5^-$ ,  $MB_5^+$ , and  $MB_5$  Species Calculated at the GIAO–B3LYP//B3LYP Method**

species	benzene	$B_5^- (C_{2v})$	$BeB_6^+$	$MgB_6^+$	$CaB_6^+$	$SrB_6^+$	$LiB_5$	$NaB_5$	$KB_5$	$RbB_5$	$CsB_5$
NICS (0.0) <sup>a</sup>	-10.13	-7.01	-17.59	-18.53	-15.04	-14.91	-9.98	-9.68	-14.98	-7.22	-5.50
NICS (0.5) <sup>b</sup>	-11.28	-15.14	-19.68	-20.41	-18.85	-18.81	-15.83	-15.66	-24.37	-6.82	-14.23

<sup>a</sup> NICS (0.0), calculated NICS values at the geometric center of the five-membered ring. <sup>b</sup> NICS (0.5), calculated NICS values above (by 0.5 Å) the geometric centers of the five-membered ring.

**Figure 3.** Molecular orbital pictures for the  $B_5^-$  anion,  $BeB_5^+$ , and  $LiB_5$  species.

supporting the existing stronger B–B bonding. The M–B bond lengths in the five  $MB_5$  and four  $MB_5^+$  species are very close to the sum of covalent radii of the corresponding metal atoms and boron atom except for  $CaB_5^+$ ,  $KB_5$ , and  $RbB_5$ . The covalent

radii for the metal atoms and boron atom were assumed to be 0.89, 1.37, 1.74, 1.91, 1.22, 1.57, 2.02, 2.16, 2.35, and 0.88 Å for Be, Mg, Ca, Sr, Li, Na, K, Rb, Cs, and B, respectively.<sup>43</sup> The calculated averaged bond lengths in the five-membered ring

for the  $MB_5^+$  and  $MB_5$  species are clearly shorter than the calculated average bond length (1.592 Å) in the most stable planar  $B_5^-$  ( $C_{2v}$ ) unit (shown in Table 2).

Figures 1 and 2 show that the  $B_5^-$  anion preserves its planar five-membered ring structural integrity in forming the  $MB_5$  ( $M = Li, Na, K, Rb,$  and  $Cs$ ) and  $MB_5^+$  ( $M = Be, Mg, Ca,$  and  $Sr$ ) species. Although in the five  $MB_5$  and four  $MB_5^+$  species, the structure of the  $B_5^-$  anion is somewhat distorted from a perfect planar five-membered ring ( $C_{2v}$ ), the distortion is very modest and the geometric integrity of the  $B_5^-$  anion is easily recognizable. Furthermore, the bond lengths of the five-membered ring are almost identical, suggesting the aromaticity of the planar  $B_5^-$  anion with structural criteria.

**3.2. Natural Population Analysis and Vibrational Frequencies.** In terms of natural population analysis, all positive charge mainly lies on the metal atoms and all negative charge populates on the boron atoms. The  $MB_5$  and  $MB_5^+$  clusters can be regarded as complexes of the  $B_5^-$  anion with the metal cations. Bonding was found to be quite ionic between the metal and  $B_5^-$ :  $Q(Be) = +1.31$  e ( $BeB_5^+$ ),  $Q(Mg) = +1.27$  e ( $MgB_5^+$ ),  $Q(Ca) = +1.62$  e ( $CaB_5^+$ ), and  $Q(Sr) = +1.66$  e ( $SrB_5^+$ ) (all are computed at the B3LYP/6-311+G\* level). With increasing atom number, the positive charges are mainly located over the metal atoms. Natural population analysis show that  $Q(Li) = +0.85$  e ( $LiB_5$ ),  $Q(Na) = +0.80$  e ( $NaB_5$ ),  $Q(K) = +0.99$  e ( $KB_5$ ),  $Q(Rb) = +0.99$  e ( $RbB_5$ ), and  $Q(Cs) = +1.00$  e ( $CsB_5$ ). At the same time, the WBI between the metal atom and boron atom in the  $LiB_5$ ,  $NaB_5$ ,  $KB_5$ ,  $RbB_5$ , and  $CsB_5$  are 0.235, 0.310, 0.026, 0.028, and 0.016, respectively. The very high ionic character in the chemical bonds of these clusters is obvious. The  $B_5^-$  anion might be stabilized as the planar five-membered ring by the interaction of its  $\pi$  system with the metal atoms. However, the metal cations have strong influences on the electronic structure of the  $B_5^-$  anion for the heavier metal atoms. So,  $RbB_5$  and  $CsB_5$  systems might change into the nonplanar structure that the five boron atoms and metal atoms are not in a plane.

The calculated harmonic vibrational frequencies at the B3LYP method for the five  $MB_5$  and four  $MB_5^+$  species are given in Table 3. The lowest vibrational frequencies calculated are large enough to prove the minimum. Whichever theoretical method was chosen, B3LYP or MP2, it made no significant difference to the vibrational frequencies for the five  $MB_5$  and four  $MB_5^+$  species.

**3.3. Aromaticity of Planar  $B_5^-$  Anion.** **3.3.1. Stabilities of the Five  $MB_5$  and Four  $MB_5^+$  Species.** The zero-point corrected B3LYP energies for hypothetical reactions  $MB_5 \rightarrow M + B_5$  ( $M = Li, Na, K, Rb,$  and  $Cs$ ) and  $MB_5^+ \rightarrow M^+ + B_5$  ( $M = Be, Mg, Ca$  and  $Sr$ ) species are given in Table 2. The  $MB_5^+$  ( $M = Be, Mg, Ca$  and  $Sr$ ) species lie about 28.7–73.8 kcal/mol above the energy of the ground-state alkaline earth metal cations  $M^+$  and the planar  $B_5$  ( $C_{2v}$ ) cluster using the B3LYP method. The  $MB_5$  ( $M = Li, Na, K, Rb,$  and  $Cs$ ) species lie about 30.3–44.3 kcal/mol above the energy of a ground-state alkali metal atoms and the planar  $B_5$  ( $C_{2v}$ ) cluster at the B3LYP method. Reactions are all endothermic, indicating that the  $MB_5$  and  $MB_5^+$  species are stable toward decomposition. Among the nine species, the  $BeB_5^+$  species is the most stable one because the reaction needs the largest energies. A simple comparison of the  $MB_5^+$  or  $MB_5$  and the planar  $B_5$  cluster energies shows a substantial energy stabilization of the  $MB_5^+$  and  $MB_5$  species.

**3.3.2. Nucleus-Independent Chemical Shifts (NICS).** Aromaticity is often discussed in terms of various criteria such as energetic, magnetic, and geometric.<sup>44–46</sup> NICS (nucleus-

independent chemical shift), proposed by Schleyer and co-workers,<sup>46</sup> is based on magnetic shieldings, which have long been calculated by simple methods,<sup>47</sup> and now can be computed with a modern ab initio technique.<sup>48</sup> NICS are computed at selected points inside or around molecules, typically at ring centers and above. Aromaticity is characterized by negative NICS values, antiaromaticity by positive NICS, and nonaromatic compounds by values close to zero.

In this study we first calculated NICS (0.0) at the geometrical centers of the planar five-membered ring, which provide a direct measure of the ring current effects. The calculated results are listed in Table 4. For the planar five-membered  $B_5^-$  structure, the NICS value of  $-7.01$  ppm computed at the center of the five-membered ring suggests that this anionic  $B_5^-$  unit is aromatic. NICS values of the nine species are all negative and larger than that of the  $B_5^-$  unit. To further analyze the aromaticity, we calculated the NICS (0.5) values by placing a ghost atom above (by 0.5 Å) the centers of the five-membered ring. NICS (0.0) and NICS (0.5) for the nine species are all negative, supporting the existence of delocalization and aromaticity of the  $B_5^-$  anion in these nine species. We found that NICS (0.0) and NICS (0.5) values for the  $MB_5^+$  ( $M = Mg, Ca,$  and  $Sr$ ) species decrease with increasing atomic number of the metal, indicating the decreasing of the aromaticity of  $MgB_5^+$ ,  $CaB_5^+$ , and  $SrB_5^+$  species. According to the NBO analysis, the calculated adjacent B–B WBI in the five-membered ring for  $B_5^-$ ,  $MB_5$ , and  $MB_5^+$  species are in the range 1.1–1.3, which are between the standard values of single-bond (1.0) and double-bond (2.0), indicating the existence of delocalization.

**3.3.3. Molecular Orbital Analysis.** As exhibited in Figure 3, the highest occupied MO (HOMO,  $1b_2$ ) of the planar  $B_5^-$  ( $C_{2v}$ ,  $^1A_1$ ) anion is a bonding orbital within the triangular wings B1–B2–B4 and B1–B3–B5 (Figure 1). The HOMO–1 ( $1a_1$ ) is formed from the in-plane p orbital and it is the peripheral four-center  $\sigma$ -bonding MO. The HOMO–2 ( $2b_2$ ) is  $\sigma$ -bonding MO formed from the in-plane p orbitals. Clearly the HOMO–3 ( $1b_1$ ), which is formed from the out-of-plane p orbitals of the five boron atoms, is a delocalized  $\pi$ -bonding MO, which renders  $\pi$ -aromaticity. The following three MOs are formed primarily from the s and p orbitals. The HOMO–7 ( $4a_1$ ) is a sum of the s orbitals of the five boron atoms. Among these occupied orbitals, the HOMO–3 ( $1b_1$ ) is a delocalized  $\pi$ -bonding MO, containing two  $\pi$  electrons. The two delocalized  $\pi$  electrons give the agreement with the  $4n + 2$  electron counting rule. Certainly, the presence of the delocalized  $\pi$  orbital plays an important role in the stabilization of this metal-polyboron species. Furthermore,  $B_5^-$  has a perfect planar ( $C_{2v}$ ) structure, due to the delocalization of  $\pi$  electrons, exactly as expected for an aromatic system.

To understand the electronic structure of the most stable  $B_5^-$  ( $C_{2v}$ ,  $^1A_1$ ) anion, we should study the electronic structure of the pentagonal  $B_5^-$  ( $D_{5h}$ ,  $^3A_1'$ ) isomer. Figure 3 shows the nine valence MOs for the pentagonal  $B_5^-$  ( $D_{5h}$ ,  $^3A_1'$ ) isomer. This triplet state is a highly symmetric pentagon with  $D_{5h}$  symmetry. As soon as the degenerate orbitals for the triplet state  $B_5^-$  ( $D_{5h}$ ) isomer are partially occupied, the Jahn–Teller distortion occurs and leads to a symmetry lowering from  $D_{5h}$  into  $C_{2v}$ . Meanwhile, the deformation causes a splitting of the degenerate orbitals transforming from  $e''$  into  $a_2$  and  $b_2$  levels.

MO pictures for  $C_{2v}$  and  $D_{5h}$   $B_5^-$  isomers show that the key orbital is HOMO–1 (Figure 3). For the singlet  $B_5^-$  with  $C_{2v}$  symmetry, the HOMO–1 ( $1a_1$ ) represents the peripheral four-center bond and the  $1a_1$  orbital is a strong bonding MO;<sup>21</sup> for triplet  $B_5^-$  with  $D_{5h}$  symmetry, the HOMO–1 ( $1a'$ ) represents

the peripheral five-center bond and is the only completely  $\sigma$ -delocalized molecular orbital to be called  $\sigma$ -aromatic.

Figure 3 also shows the eight valence MOs for  $\text{BeB}_5^+$  and  $\text{LiB}_5$ . The canonical MO ordering of  $\text{BeB}_5^+$  and  $\text{LiB}_5$  is different from that of  $\text{B}_5^-$ . In the  $\text{BeB}_5^+$  and  $\text{LiB}_5$  species the MOs of the  $\text{B}_5^-$  anion can be easily recognized. They only distort slightly by the presence of the metal cations, exhibiting the electronic integrity of the  $\text{B}_5^-$  anion. We found that a similar delocalized  $\pi$  orbital and the peripheral four-center bond are also present in the  $\text{BeB}_5^+$  and  $\text{LiB}_5$  species, showing the electronic integrity of the  $\text{B}_5^-$  anion. The other  $\text{MB}_5^+$  and  $\text{MB}_5$  species also have similar MO pictures.

Molecular orbital analysis for the  $\text{B}_5^-$  anion revealed an interesting and delocalized  $\pi$  MO. They contribute the property of the  $\pi$ -aromaticity for the  $\text{B}_5^-$  anion, due to the presence of two  $\pi$  electrons which follow the  $4n + 2$  electron counting rule.

#### 4. Conclusion

In this paper, the equilibrium geometries and harmonic vibrational frequencies of the low-lying states of alkali metal– $\text{B}_5^-$   $\text{MB}_5$  ( $M = \text{Li, Na, K, Rb, and Cs}$ ) and alkaline earth metal– $\text{B}_5^-$   $\text{MB}_5^+$  ( $M = \text{Be, Mg, Ca, and Sr}$ ) clusters are discussed for the first time. Comprehensive calculations show that the planar  $\text{B}_5^-$  anion can coordinate with one metal atom to form  $\text{MB}_5$  and  $\text{MB}_5^+$ . First, the presence of two delocalized  $\pi$  electrons of  $\text{B}_5^-$  anion satisfies the  $4n + 2$  electron counting rule, exhibiting characteristics of  $\pi$ -aromaticity for the  $\text{B}_5^-$  anion. Second,  $\text{B}_5^-$  has a planar five-member ring structure, due to the delocalized  $\pi$  electrons. Third, NICS and WBI values suggest the property of aromaticity of the  $\text{B}_5^-$  anion. Finally, the structural and electronic integrity of the  $\text{B}_5^-$  anion inside the  $\text{MB}_5^+$  and  $\text{MB}_5$  species can be presented. Therefore, the planar cyclic  $\text{B}_5^-$  anion exhibits characteristics of  $\pi$ -aromaticity and maintains its structural and electronic integrity inside of the  $\text{MB}_5$  and  $\text{MB}_5^+$  species. These findings are significant for expanding the aromaticity concept into inorganic  $\text{B}_5^-$  cluster.

#### References and Notes

- Hanley, L.; Whitten, J. L.; Anderson, S. L. *J. Phys. Chem.* **1988**, *92*, 5803.
- Ruatta, S. A.; Hanley, L.; Anderson, S. L. *J. Chem. Phys.* **1989**, *91*, 226.
- Hintz, P. A.; Ruatta, S. A.; Anderson, S. L. *J. Chem. Phys.* **1990**, *92*, 292.
- Ruatta, S. A.; Hintz, P. A.; Anderson, S. L. *J. Chem. Phys.* **1991**, *94*, 2833.
- Hintz, P. A.; Sowa, M. B.; Ruatta, S. A.; Anderson, S. L. *J. Chem. Phys.* **1991**, *94*, 6446.
- Bruna, P. J.; Wright, J. S. *J. Phys. Chem.* **1990**, *94*, 1774; *J. Mol. Struct.* **1990**, *210*, 243; *J. Chem. Phys.* **1989**, *91*, 1126; *J. Chem. Phys.* **1990**, *93*, 2617.
- Niu, J.; Rao, B. K.; Jena, P. *J. Chem. Phys.* **1997**, *107*, 132.
- Langhoff, S. R.; Bauschlicher, C. W. *J. Chem. Phys.* **1991**, *95*, 5882.
- Kimura, K.; Takeda, M.; Fujimori, M.; Tamura, R.; Matsuda, H.; Schmechel, R.; Werheit, H. *J. Solid State Chem.* **1997**, *133*, 302.
- Hernandez, R.; Simons, J. *J. Chem. Phys.* **1991**, *94*, 2961.
- Ray, A. K.; Howard, I. A.; Kanal, K. M. *Phys. Rev. B* **1992**, *45*, 14247.
- Kato, A. U.; Yamashita, K.; Morokuma, K. *Chem. Phys. Lett.* **1992**, *190*, 361.
- Boustani, I. *Surf. Sci.* **1996**, *370*, 355; *Int. J. Quantum Chem.* **1994**, *52*, 1081; *Chem. Phys. Lett.* **1995**, *233*, 273; *Chem. Phys. Lett.* **1995**, *240*, 135; *Phys. Rev. B* **1997**, *55*, 16426.
- Tang, A. C.; Li, Q. S. *Int. J. Quantum Chem.* **1986**, *29*, 579.
- Tang, A. C.; Li, Q. S.; Liu, C. W.; Li, J. *Chem. Phys. Lett.* **1993**, *201*, 465.
- Li, Q. S.; Gu, F. L.; Tang, A. C. *Int. J. Quantum Chem.* **1994**, *50*, 173.
- Jin, H. W.; Li, Q. S. *Phys. Chem. Chem. Phys.* **2003**, *5*, 1110.
- Li, Q. S.; Jin, H. W. *J. Phys. Chem. A* **2002**, *106*, 7042.
- Alexandrova, A. N.; Boldyrev, A. I.; Zhai, H. J.; Wang, L. S.; Steiner, E.; Fowler, P. W. *J. Phys. Chem. A* **2003**, *107*, 1359.
- Ma, J.; Li, Z. H.; Fan, K. N.; Zhou, M. F. *Chem. Phys. Lett.* **2003**, *372*, 708.
- Zhai, H. J.; Wang, L. S.; Alexandrova, A. N.; Boldyrev, A. I. *J. Chem. Phys.* **2002**, *117*, 7917.
- Li, X.; Kuznetsov, A. E.; Zhang, H. F.; Boldyrev, A. I.; Wang, L. S. *Science* **2001**, *291*, 859.
- Kuznetsov, A. E.; Boldyrev, A. I.; Li, X.; Wang, L. S. *J. Am. Chem. Soc.* **2001**, *123*, 8825.
- Li, X.; Zhang, H. F.; Wang, L. S.; Kuznetsov, A. E.; Cannon, N. A.; Boldyrev, A. I. *Angew. Chem., Int. Ed.* **2001**, *40*, 1867.
- Kuznetsov, A. E.; Boldyrev, A. I. *Struct. Chem.* **2002**, *13*, 141.
- Alexandrova, A. N.; Boldyrev, A. I. *J. Phys. Chem. A* **2003**, *107*, 554.
- Kuznetsov, A. E.; Wang, L. S.; Corbett, J. D.; Boldyrev, A. I. *Angew. Chem., Int. Ed.* **2001**, *40*, 3369.
- Boldyrev, A. I.; Kuznetsov, A. E. *Inorg. Chem.* **2002**, *41*, 532.
- Kuznetsov, A. E.; Boldyrev, A. I.; Zhai, H. J.; Li, X.; Wang, L. S. *J. Am. Chem. Soc.* **2002**, *124*, 11791.
- Li, X.; Wang, L. S.; Boldyrev, A. I.; Simons, J. *J. Am. Chem. Soc.* **1999**, *121*, 6033.
- Wang, L. S.; Boldyrev, A. I.; Li, X.; Simons, J. *J. Am. Chem. Soc.* **2000**, *122*, 7681.
- Kuznetsov, A. E.; Alexander Birch, K.; Boldyrev, A. I.; Li, X.; Zhai, H. J.; Wang, L. S. *Science* **2003**, *300*, 622.
- Li, Q. S.; Cheng, L. P. *J. Phys. Chem. A* **2003**, *107*, 2882.
- Frisch, M. J.; Trucks, G. W.; Schlegel, H. B.; Scuseria, G. E.; Robb, M. A.; Cheeseman, J. R.; Zakrzewski, V. G.; Montgomery, J. A., Jr.; Stratmann, R. E.; Burant, J. C.; Dapprich, S.; Millam, J. M.; Daniels, A. D.; Kudin, K. N.; Strain, M. C.; Farkas, O.; Tomasi, J.; Barone, V.; Cossi, M.; Cammi, R.; Mennucci, B.; Pomelli, C.; Adamo, C.; Clifford, S.; Ochterski, J.; Petersson, G. A.; Ayala, P. Y.; Cui, Q.; Morokuma, K.; Malick, D. K.; Rabuck, A. D.; Raghavachari, K.; Foresman, J. B.; Cioslowski, J.; Ortiz, J. V.; Baboul, A. G.; Stefanov, B. B.; Liu, G.; Liashenko, A.; Piskorz, P.; Komaromi, I.; Gomperts, R.; Martin, R. L.; Fox, D. J.; Keith, T.; Al-Laham, M. A.; Peng, C. Y.; Nanayakkara, A.; Challacombe, M.; Gill, P. M. W.; Johnson, B.; Chen, W.; Wong, M. W.; Andres, J. L.; Gonzalez, C.; Head-Gordon, M.; Replogle, E. S.; Pople, J. A. *Gaussian 98*, Revision A.9; Gaussian, Inc.: Pittsburgh, PA, 1998.
- Hehre, W. J.; Radom, L.; Schleyer, P. v. R.; Pople, J. A. *Ab initio Molecular Orbital Theory*; Wiley: New York, 1986.
- Becke, A. D. *J. Chem. Phys.* **1993**, *98*, 5648.
- Lee, C.; Yang, W.; Parr, R. G. *Phys. Rev. B* **1988**, *37*, 785.
- Schaftenaar, G. *MOLDEN 3.4*. CAOS/CAMM Center, The Netherlands, 1998.
- Carpenter, J. E.; Weinhold, F. *J. Mol. Struct. (THEOCHEM)* **1988**, *169*, 41.
- Foster, J. P.; Weinhold, F. *J. Am. Chem. Soc.* **1980**, *102*, 7211.
- Reed, A. E.; Curtiss, L. A.; Weinhold, F. *Chem. Rev.* **1988**, *88*, 899.
- Reed, A. E.; Weinstock, R. B.; Weinhold, F. *J. Chem. Phys.* **1985**, *83*, 735.
- Periodic Table of Elements*; Wiley-VCH: Weinheim, 1997.
- Schleyer, P. v. R.; Subramanian, G.; Jiao, H.; Najafian, K.; Hofmann, M. *In Advances in Boron Chemistry*; Siebert, W., Eds.; Royal Society of Chemistry: Cambridge, U.K., 1997; p 1–14.
- (a) Schleyer, P. v. R.; Najafian, K. Are Polyhedral Boranes, Carboranes, and Carbocations Aromatic? In *The Borane, Carborane, Carbocation Continuum*; Casanova, J., Ed.; Wiley: New York, 1998; pp 169–190. (b) Schleyer, P. v. R.; Najafian, K. *Inorg. Chem.* **1998**, *37*, 3454.
- (a) Hofmann, M.; Schleyer, P. v. R. *Inorg. Chem.* **1999**, *38*, 652. (b) Unverzagt, M.; Winkler, H. J.; Brock, M.; Hofmann, M.; Schleyer, P. v. R.; Massa, W.; Berndt, A. *Angew. Chem., Int. Ed. Engl.* **1997**, *36*, 853. (c) Schleyer, P. v. R.; Jiao, H.; Hommes, N. J. R. v. E.; Malkin, V. G.; Malkina, O. L. *J. Am. Chem. Soc.* **1997**, *119*, 12669.
- Pasquarello, A.; Schlüter, M.; Haddon, R. C. *Science* **1992**, *257*, 1660.
- Schleyer, P. v. R.; Maerker, C.; Dransfeld, A.; Jiao, H.; Hommes, N. J. R. v. E. *J. Am. Chem. Soc.* **1996**, *118*, 6317.